Texture inheritance in thin-film growth of Cu_2ZnSnS_4

A. Weber, S. Schmidt, D. Abou-Ras, P. Schubert-Bischoff, I. Denks, R. Mainz, and H. W. Schock

Texture inheritance in thin-film growth of Cu$_2$ZnSnS$_4$

A. Weber,[a)] S. Schmidt, D. Abou-Ras, P. Schubert-Bischoff, I. Denks, R. Mainz, and H. W. Schock

Helmholtz-Zentrum Berlin für Materialien und Energie, Glienicker Str. 100, D-14109 Berlin, Germany

The growth mechanism of Cu$_2$ZnSnS$_4$ thin films is studied starting from highly textured ZnS precursor films. These precursors were converted to Cu$_2$ZnSnS$_4$ by subsequent deposition of Cu, Sn, and S at high temperatures. Orientation measurements revealed that the $\langle 111 \rangle$ texture of the ZnS precursor is inherited by the Cu$_2$ZnSnS$_4$ layer. On the basis of texture and transmission electron microscopy measurements, a growth model is proposed. According to this model, the initial formation of Cu$_2$ZnSnS$_4$ nuclei is controlled by a topotactic or epitactic mechanism with respect to the ZnS precursor. The further growth of the Cu$_2$ZnSnS$_4$ grains appears to be independent of the precursor lattice. © *2009 American Institute of Physics*. [DOI: 10.1063/1.3192357]

Cu$_2$ZnSnS$_4$ is a promising thin-film photovoltaic absorber material and the best solar cells of this compound have recently reached conversion efficiencies of 6.7%.[1] The thermodynamically most stable crystal structure of Cu$_2$ZnSnS$_4$ is kesterite (space group $I\bar{4}$),[2] which is similar to the chalcopyrite structure of Cu(In,Ga)Se$_2$ (space group $I\bar{4}2d$).[3] The latter compound is a well known photovoltaic absorber material, reaching efficiencies of up to 20%.[4] The best absorber layers are formed in evaporation processes where a precursor layer of (In,Ga)$_2$Se$_3$ is transformed to Cu(In,Ga)Se$_2$ (Refs. 5 and 4) in (Cu+Se) flux. It has been found earlier that a texture of the precursor layer also leads to a texture in the resulting absorber layer.[6] This texture inheritance has been explained by the structural similarity of In$_2$Se$_3$ and CuInSe$_2$. A similar effect has been proposed for the phase Cu$_{2-x}$Se,[7–9] which is formed in Cu-rich films. These findings have led to the model that CuInSe$_2$ (Ref. 8) and Cu(In,Ga)Se$_2$ (Ref. 9) can be grown from the precursor phases by a topotactic mechanism. This mechanism implies that the crystalline lattice and orientation of the precursor remain mostly unchanged, while only the atoms of specific lattice sites are exchanged.[10] A topotactic mechanism is also plausible for the growth of Cu$_2$ZnSnS$_4$ from the precursors ZnS and Cu$_2$SnS$_3$.[11] These three phases can crystallize in the structure or a superstructure of sphalerite.[12–15] In this letter we investigate the formation of Cu$_2$ZnSnS$_4$ starting from a ZnS precursor in order to clarify the atomistic mechanism of the reaction.

Precursor deposition and the subsequent transformation to Cu$_2$ZnSnS$_4$ were carried out in a physical vapour deposition system described elsewhere.[16] Three ZnS precursors were deposited by evaporating ZnS on Mo-coated soda lime glass substrates. The substrate temperature was approximately 420 K. After deposition of the ZnS layer, the three substrates were heated to 650 K and at constant temperature Cu, Sn, and S were evaporated simultaneously on the substrates. Earlier experiments[16] had revealed a low Sn adsorption at these temperatures. Therefore a high Sn/Cu evaporation ratio of approximately 1 was applied to avoid Sn deficiency in the layers. After defined periods of the evapo-

ration process, the three substrates were successively removed from the deposition zone with a manipulator and cooled down rapidly. The morphology of the processed films was analyzed with a scanning electron microscope (SEM, LEO1530 Gemini). Texture measurements were performed on a diffractometer (Seifert MZ VI, tilting angle: $85° > \psi > 0°$ rotation angle: $355° > \phi > 0°$, step width: 5°). The depth profile of the elemental composition was measured by energy dispersive x-ray spectroscopy (EDX) in scanning mode on a transmission electron microscope (STEM) (Zeiss Libra 200FE). The same microscope was used for high resolution TEM (HRTEM) micrographs.

Figure 1 shows cross sections of the films after different deposition times. After 2.5 and 5.5 min evaporation, a bottom layer with columnar grains and high contrast in the SEM picture can be observed. Grains with significantly different SEM contrast and morphology can be found on top of this layer. After 20.5 min, the bottom layer has disappeared.

To clarify the observed differences in the SEM contrast of the different layers, a STEM-EDX depth profile was measured. Figure 2 shows the result of an EDX linescan along the cross section of sample (b) from Fig. 1. In the top layer Cu, Zn and Sn are homogeneously distributed throughout the depth of the layer. In the bottom layer, the Zn signal is strong and the Sn signal and Cu signal are in the range of the detection limit. The S signal is approximately constant throughout the layer. In diffraction measurements on this layer (not presented here), the kesterite superstructure reflexes could be identified clearly. From these results we derive that the top layer consists of Cu$_2$ZnSnS$_4$ while the bottom layer repre-

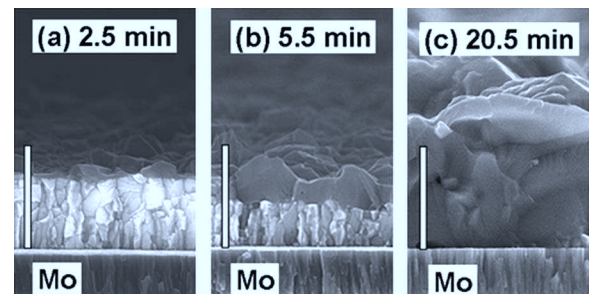FIG. 1. SEM micrographs on cross sections of the ZnS precursors after different times of (Cu+Sn+S) evaporation at 650 K. The bars mark 1 μm.
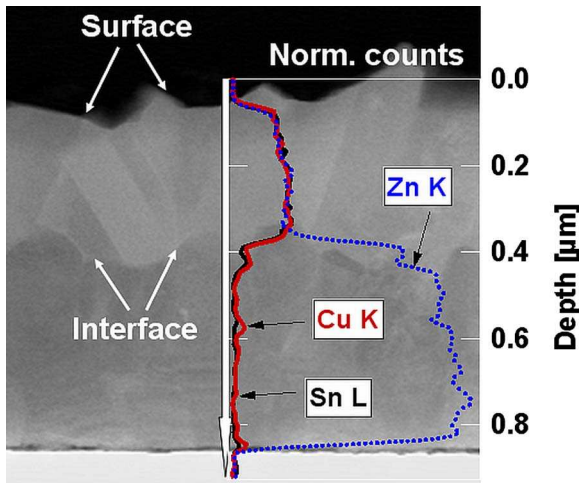
a)Electronic mail: alfons.weber@helmholtz-berlin.de.

FIG. 2. (Color online) STEM-EDX depth profile on a cross section of the ZnS precursor after 5.5 min of (Cu+Sn+S) evaporation.

FIG. 4. (Color online) Pole figures for different diffracting planes of the Cu_2ZnSnS_4 layer after 20.5 min of (Cu+Sn+S) evaporation. The intensity rings indicate a double fiber texture in the directions $\langle 111 \rangle$ and $\langle 100 \rangle$.

sents the unreacted precursor ZnS. In combination with Fig. 1, we conclude that the layers consist mainly of ZnS after 2.5 min and mainly of Cu_2ZnSnS_4 after 20.5 min of (Cu+Sn+S) evaporation. This is confirmed by diffraction measurements where after 20.5 min, the typical kesterite diffraction pattern[12] could be found (not presented here).

In case of a topotactic formation of Cu_2ZnSnS_4 from ZnS, the orientations of the precursor grains and of the Cu_2ZnSnS_4 grains are identical. A texture of the precursor layer would therefore also result in a comparable texture of the Cu_2ZnSnS_4 layer. Figure 3 shows the result of a texture measurement on the ZnS precursor after 2.5 min of (Cu+Sn+S) evaporation. The measured figures are typical for a $\langle 111 \rangle$ fiber texture of a cubic crystal structure.

The same measurement was performed for the ZnS precursor after 20.5 min of (Cu+Sn+S) evaporation, i.e., for the Cu_2ZnSnS_4 (kesterite) layer. Kesterite is a tetragonally distorted superstructure of the cubic sphalerite, for reasons of simplification the {112} planes of this system will be treated as $\{111\}_{cub}$ and the {200}/{004} planes as $\{200\}_{cub}$. The resulting pole figures in Fig. 4 can be well explained by a double fiber texture in the directions $\langle 111 \rangle_{cub}$ and $\langle 100 \rangle_{cub}$.

On first sight, the pole figure measurements seem to prove a topotactic reaction mechanism because the $\langle 111 \rangle$ fiber texture is inherited from the precursor to the product layer. But the formation of an additional $\langle 100 \rangle$ fiber texture cannot be explained by this model. To clarify these contradicting findings, we investigated the interface between the

ZnS precursor and the Cu_2ZnSnS_4 layer with HRTEM. Figure 5 shows a HRTEM micrograph of this interface for the sample after 5.5 min of (Cu+Sn+S) evaporation. The lattice planes of two ZnS grains can be discerned, with plane distances of about 0.3 nm and an intersecting angle of the planes of about 109°. These planes are therefore identified as {111} sphalerite planes. For the Cu_2ZnSnS_4 grain, only one set of planes can be observed. These planes are tilted more than 15° with respect to the ZnS planes. Two further measurements at different locations of the interface also showed no exact match between the orientations of ZnS grains and Cu_2ZnSnS_4 grains.

Because of (i) the different morphology of precursor and product, (ii) the appearance of an additional texture during processing, and (iii) the missing coherence of the lattice orientations of neighboring precursor grains and product grains, we assume that film growth is not solely based on a topotactic mechanism. We suggest the following growth model: in an initial stage, Cu_2ZnSnS_4 nuclei are formed on top of the ZnS layer. Via a topotactic or epitactic mechanism of the nucleation step, the underlying textured ZnS grains will induce preferably a $\langle 111 \rangle_{cub}$ orientation in the nuclei. To some extent also $\langle 100 \rangle_{cub}$ orientation will occur which may be due to a structural relationship between the $\langle 111 \rangle_{cub}$ and $\langle 100 \rangle_{cub}$ direction. With further processing the Cu_2ZnSnS_4 grains enlarge and overgrow neighboring ZnS grains. As neighboring ZnS grains exhibit a certain misorientation, incoherent $ZnS-Cu_2ZnSnS_4$ interfaces will necessarily form. The further formation of Cu_2ZnSnS_4 in the film is most likely not controlled by the precursor lattice but by material transport through the already grown Cu_2ZnSnS_4 layer. This letter
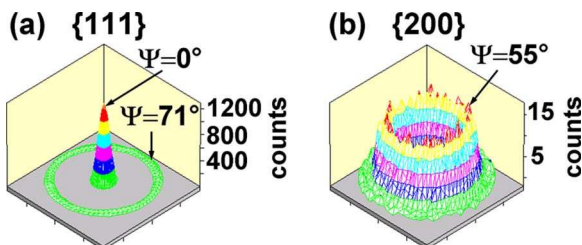

FIG. 3. (Color online) Pole figures for different diffracting planes of the ZnS precursor after 2.5 min of (Cu+Sn+S) evaporation. The intensity rings are typical for a $\langle 111 \rangle$ fiber texture in a cubic system (theoretical interplanar angle of {111} planes: 70.5°, theoretical interplanar angle of {111} and {200} planes: 54.7°).
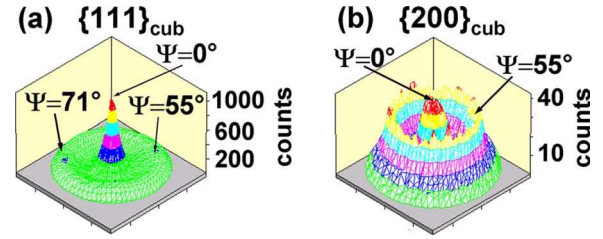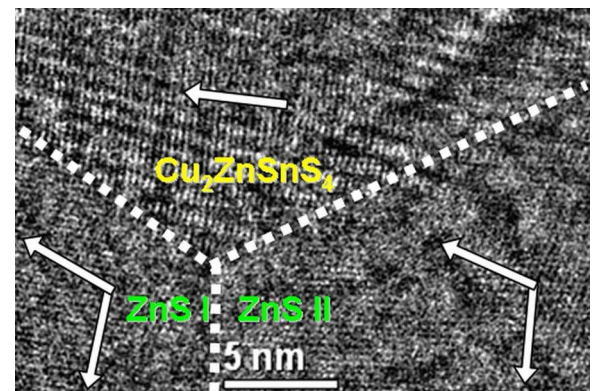

FIG. 5. (Color online) HRTEM micrograph of the $ZnS-Cu_2ZnSnS_4$ interface after 5.5 min of processing. The arrows mark the normals of the observed lattice planes. The dotted lines mark the grain boundaries. The planes of the Cu_2ZnSnS_4 grain are tilted more than 15° with respect to the ZnS planes.

shows that a texture inheritance from the precursor is not necessarily coupled with an exclusively topotactic mechanism of the underlying chemical reaction.

[1]H. Katagiri, K. Jimbo, S. Yamada, T. Kamimura, W. S. Maw, T. Fukano, T. Ito, and T. Motohiro, Appl. Phys. Express **1**, 041201 (2008).

[2]S. Chen, X. G. Gong, A. Walsh, and S. H. Wie, Appl. Phys. Lett. **94**, 041903 (2009).

[3]S. Schorr, Thin Solid Films **515**, 5985 (2007).

[4]M. A. Contreras, K. Ramanathan, J. A. Shama, F. Hasoon, D. L. Young, B. Egass, and R. Noufi, Prog. Photovoltaics **13**, 209 (2005).

[5]S. Zweigart, S. M. Sun, G. Bilger, and H. W. Schock, Sol. Energy Mater. Sol. Cells **41**, 219 (1996).

[6]M. A. Contreras, B. Egaas, D. King, A. Swartzlander, and T. Dullweber, Thin Solid Films **361–362**, 167 (2000).

[7]R. Klenk, T. Walter, H. W. Schock, and D. Cahen, Adv. Mater. **5**, 114 (1993).

[8]T. Wada, N. Kohara, T. Negami, and M. Nishitani, J. Mater. Res. **12**, 1456 (1997).

[9]F. Hergert, S. Jost, R. Hock, and M. Purwins, J. Solid State Chem. **179**, 2394 (2006).

[10]R. D. Shannon and R. C. Rossi, Nature (London) **202**, 1000 (1964).

[11]F. Hergert and R. Hock, Thin Solid Films **515**, 5953 (2007).

[12]S. R. Hall, J. T. Szymanski, and J. M. Stewart, Can. Mineral. **16**, 131 (1978).

[13]M. Onoda, X. Chen, M. Sato, and H. Wada, Mater. Res. Bull. **35**, 1563 (2000).

[14]J. C. Jamieson and H. H. Demarest, J. Phys. Chem. Solids **41**, 963 (1980).

[15]C. Y. Yeh, Z. W. Lu, S. Froyen, and A. Zunger, Phys. Rev. B **46**, 10086 (1992).

[16]A. Weber, H. Krauth, S. Perlt, B. Schubert, I. Kötschau, S. Schorr, and H. W. Schock, Thin Solid Films **517**, 2524 (2009).